Journal of Marine Science and Technology

Volume 25 | Issue 2 Article 2

FINITE ELEMENT METHOD IN STATISTICAL ANALYSIS OF FLEXIBLE PAVEMENT

Abdollah Shayesteh
Department of Civil Engineering, Marivan Branch, Islamic Azad University, Marivan, Iran., k.keyvani2000@gmail.com

Elahe Ghasemisalehabadi
Department of Civil Engineering, Payame Noor University, Tehran, Iran.

Mohammad Worya Khordehbinan
Department of Civil Engineering, Payame Noor University, Tehran, Iran.

Touba Rostami
Department of Civil Engineering, Marivan Branch, Islamic Azad University, Marivan, Iran.

Recommended Citation
Shayesteh, Abdollah; Ghasemisalehabadi, Elahe; Khordehbinan, Mohammad Worya; and Rostami, Touba (2017) "FINITE ELEMENT METHOD IN STATISTICAL ANALYSIS OF FLEXIBLE PAVEMENT," *Journal of Marine Science and Technology*: Vol. 25: Iss. 2, Article 2.
DOI: 10.6119/JMST-016-0721-1
Available at: https://jmstt.ntou.edu.tw/journal/vol25/iss2/2

FINITE ELEMENT METHOD IN STATISTICAL ANALYSIS OF FLEXIBLE PAVEMENT

Acknowledgements

This work was financially supported by Islamic Azad University, Marivan Branch, Marivan, Iran.

Journal of Marine Science and Technology, Vol. 25, No. 2, pp. 142-152 (2017)
DOI: 10.6119/JMST-016-0721-1

FINITE ELEMENT METHOD IN STATISTICAL ANALYSIS OF FLEXIBLE PAVEMENT

Abdollah Shayesteh[1], Elahe Ghasemisalehabadi[2],
Mohammad Worya Khordehbinan[2], and Touba Rostami[1]

Key words: flexible pavement, finite element, cross-anisotropic, KENLAYER, ABAQUS.

ABSTRACT

In this paper, we first compare pavement analysis methods, namely the finite element (FE) method with ABAQUS software and the theory of multilayer systems with KENLAYER software. Second, the FEs identified in the pavement analysis are used to study the effect of isotropic material features in pavement reactions to traffic loads. We found that the results of the FE analysis accorded with those derived from the theory of multilayer systems, with no significant difference among the mean values obtained using both techniques. The findings show that, the anisotropic properties of materials have no significant effect on the magnitude of pavement displacement under traffic loads, while have significant effect on the magnitude of tensile strain. Thus, the anisotropic properties of materials should be considered when modeling pavement structures.

I. INTRODUCTION

Methods applied for pavement must be perfectly proportional with the environment pavement construction. Flexible pavement consists of a subbase course and base materials that are anisotropic, including hot-mix asphalt (HMA). Soil particle orientation after compaction is the major factor determining the anisotropic behavior of stabilized and nonstabilized pavement materials (Oda et al., 1985; Oda and Nakayama, 1989). Therefore, the anisotropic characteristic of soil depends on the degree of compaction (Brown et al., 1989). Tutumluer (1955) concluded that compaction-induced stress is another factor affecting the degree of anisotropic behavior in soil materials. Stress from traffic loading and compaction of the pavement layer cause soil particles to slide over each other and change orientation. This may comminute soil particles and render the soil prone to anisotropic behavior. Tutumluer et al. (2003) stated that the modulus of elasticity of soil structures changes with the orientation of soil particles. Thus, the modulus of elasticity in the horizontal direction may be lower than that in the vertical direction; if this is not considered when analysing pavement structures, the values of the stress induced in the materials might be unrealistic. Studies on the anisotropic behavior of the course materials in the subbase and base of pavement systems have shown that it is appropriate to characterize these materials as anisotropic and to consider them as stress sensitive when describing their behavior (Chan and Brown, 1994; Brown, 1996; Tutumluer, 1998; Adu-Osei et al., 2000; Tutumler et al., 2003). In cross-anisotropic modeling of pavement systems with the finite element (FE) method, obtaining accurate input parameters values is critical for modeling the system as anisotropic. Notably, the International Center for Aggregate Research provided a method for obtaining accurate parameter values (Chan and Brown, 1994; Kolisoja, 1997; Adu-Osei et al., 2000).

Asphalt concrete mixture consists of aggregates, bitumen, and fillers. Because aggregates exhibit anisotropic behavior, asphalt concrete also exhibits anisotropic behavior (Wang and Hoyos, 2004). Bitumen is an adhesive homogeneous material that reduces the anisotropic behavior of asphalt concrete mixture. The results of numerous studies on the anisotropic properties of asphalt concrete have shown that the asphalt concrete exhibits anisotropic behavior. Wagoner and Braham (2008) studied the anisotropic behavior of asphalt mix at low temperatures; after performing tests to determine the complex modulus, creep compliance, and tensile strength, they concluded that asphalt concrete exhibits anisotropic behavior at low temperatures, although the tensile strength of the material does not depend on the orientation of the particles. According to Underwood et al. (2005), Heidari has performed several tests in this field, evidencing that the anisotropic properties of asphalt concrete decrease at high temperatures.

According to extant research, the affect of the anisotropic properties of pavement materials on the critical responses of pavement structures to traffic loads has not been well determined. A shortcoming of most studies cited in the present study is that their findings have been inconsistent because the

Paper submitted 06/13/16; revised 07/27/15 ; accepted 07/21/16. Author for correspondence: Abdollah Shayesteh (e-mail: k.keyvani2000@gmail.com).
[1] Department of Civil Engineering, Marivan Branch, Islamic Azad University, Marivan, Iran.
[2] Department of Civil Engineering, Payame Noor University, Tehran, Iran.

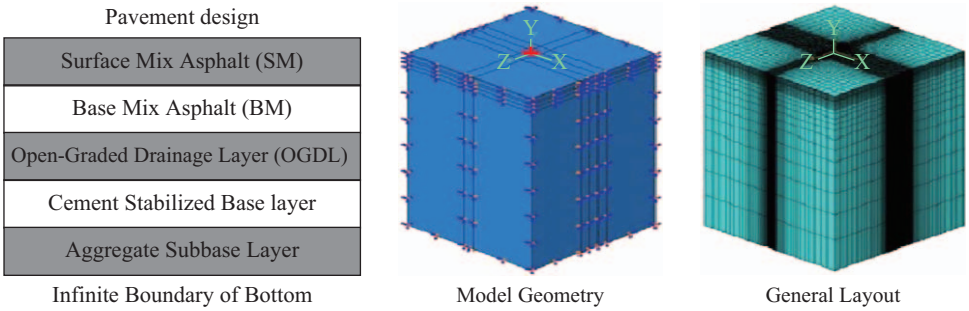

Fig. 1. 3D FE model.

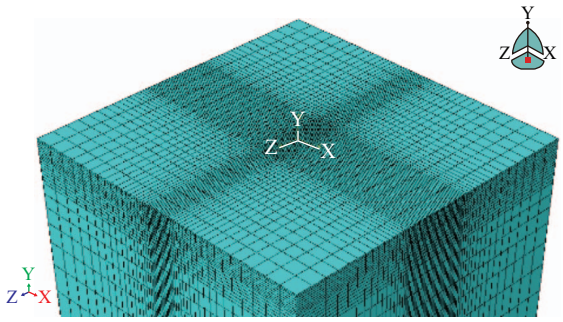

Fig. 2. Fine mesh in the load region.

anisotropic effect of soil and asphalt layers have not been considered simultaneously. However, in this present study on predicting the critical responses of pavement structures, the anisotropic properties of soil and asphalt layers were considered simultaneously.

II. 3D FE MODELING AND VALIDATION

In this study, the commercial software ABAQUS version 6.11 was used for 3D FE to model the pavement. Al-Qadi et al. (2002) measured responses of pavement to the new generation of wide-base tires at the Virginia Smart Road test-bed facility. Measured stresses and strains have been applied to investigate the effect of various adoptive parameters on pavement response (Al-Qadi et al., 2004a, 2004b, 2005). All pavement models in this study simulated the pavement design of Section B at the Virginia Smart Road test-bed facility.

In the FE model, the width of each layer was assumed to be 3650 mm according to the pavement structure. Selecting the appropriate element type is a critical step in FE modeling; ABAQUS provides a diverse element library. An earlier study successfully employed an eight-node linear brick element in a pavement response analysis. To improve the convergence rate, eight-node linear brick elements with reduced integration (i.e., C3D8R) for various thicknesses were selected. A generated 3D mesh was designed to provide optimal accuracy for finer elements in regions requiring detailed load modeling and relatively large elements far from the loading area. Fig. 1 shows the general layout of the developed 3D FE model. The large elements in the model measured 1.231 m, and those in the load region measured 0.02053 m; fine mesh was used in the load region and coarse mesh was used at a distance from the load region. Fig. 2 shows the fine mesh in the load region. A total of 108630 elements were used, and a mesh convergence study was conducted to determine the optimum number of elements.

This study was conducted for two main purposes: (a) compare two pavement anaylsis methods, namely FE pavement analyses with ABAQUS software and the theory of multilayer system with KENLAYER software and (b) examine the FEs of the pavement analysis and study the effect of the isotropic material features on the pavement response to load.

In the first part of this study, all layers were modeled in a linear elastic system. For the second part, all pavement layers were modeled and analyzed in both isotropic and cross-anisotropic systems.

1. Material Characterization for Modeling the Elastic and Isotropic Systems

Material characterization of the pavement materials was obtained through nondestructive testing of pavement layers as well as from laboratory test results from Section B of the Virginia Smart Road test-bed facility (Al-Qadi et al., 2002). The elastic moduli of the subgrade layers were calculated using the falling weight deflectometer (FWD) deflection basin. The back-calculation software MICHBACK was employed to perform FWD tests after modeling each layer. The calculated subgrade modulus was then applied as a seed value in ABAQUS to determine the elastic moduli for the other layers, namely the open-graded drainage layer, cement-treated base, and granular subbase. The resilient modulus test for HMA was performed at a temperature of 25°C; the results are presented in Table 1.

2. Material Characterization for Modeling the Anisotropic System

In the isotropic model, the elastic properties of the material, such as the elasticity modulus and Poisson's constant, are identical in all directions. This model has been used in numerous pavement analysis models. In the present model, the strain-stress formula is expressed as follows (ABAQUS User Manual, 2014):

Table 1. Back calculated pavement moduli.

Layer	Layer Thickness (mm)	Young's Modulus (MPa)	Poisson's Ratio
Surface Mix(SM)	38	*4230*	0.33
Base Mix (BM)	150	4750	0.30
open-graded drainage layer (OGDL)	75	2415	0.30
Cement Stabilized Base	150	11000	0.25
Aggregate Subbase Layer	175	310	0.35
Subgrade	Infinite	262	0.35

$$\begin{Bmatrix}\varepsilon_{11}\\ \varepsilon_{22}\\ \varepsilon_{33}\\ \gamma_{12}\\ \gamma_{13}\\ \gamma_{23}\end{Bmatrix}=\begin{bmatrix}\frac{1}{E} & \frac{-\nu}{E} & \frac{-\nu}{E} & 0 & 0 & 0\\ \frac{-\nu}{E} & \frac{1}{E} & \frac{-\nu}{E} & 0 & 0 & 0\\ \frac{-\nu}{E} & \frac{-\nu}{E} & \frac{1}{E} & 0 & 0 & 0\\ 0 & 0 & 0 & \frac{1}{G} & 0 & 0\\ 0 & 0 & 0 & 0 & \frac{1}{G} & 0\\ 0 & 0 & 0 & 0 & 0 & \frac{1}{G}\end{bmatrix}\begin{Bmatrix}\sigma_{11}\\ \sigma_{22}\\ \sigma_{33}\\ \sigma_{12}\\ \sigma_{13}\\ \sigma_{23}\end{Bmatrix}$$

where

σ_{ij}: Vertical stress on plane ij
ε_{ij}: Vertical strain on plane ij
γ_{ij}: Shear strain on plane ij
E: Elasticity city modulus
ν: Poisson's constant
G: Shear modulus, calculated as $G=\dfrac{E}{2(1+\theta)}$

In the anisotropic model, the properties of the materials differ among the three axes. Because of the numerus parameters in this model and the difficulty involved in determining these parameters, this model is rarely used in pavement analyses. In this model, the stress-strain formula is expressed as follows (ABAQUS User Manual, 2014):

$$\begin{Bmatrix}\varepsilon_{11}\\ \varepsilon_{22}\\ \varepsilon_{33}\\ \gamma_{12}\\ \gamma_{13}\\ \gamma_{23}\end{Bmatrix}=\begin{bmatrix}\frac{1}{E_1} & \frac{-\nu_{21}}{E_2} & \frac{-\nu_{31}}{E_3} & 0 & 0 & 0\\ \frac{-\nu_{12}}{E_1} & \frac{1}{E_2} & \frac{-\nu_{32}}{E_3} & 0 & 0 & 0\\ \frac{-\nu_{13}}{E_1} & \frac{-\nu_{23}}{E_2} & \frac{1}{E_3} & 0 & 0 & 0\\ 0 & 0 & 0 & \frac{1}{G_{12}} & 0 & 0\\ 0 & 0 & 0 & 0 & \frac{1}{G_{13}} & 0\\ 0 & 0 & 0 & 0 & 0 & \frac{1}{G_{23}}\end{bmatrix}\begin{Bmatrix}\sigma_{11}\\ \sigma_{22}\\ \sigma_{33}\\ \sigma_{12}\\ \sigma_{13}\\ \sigma_{23}\end{Bmatrix}$$

where

E_{ij}: Elasticity modulus along axis i
ν_{ij}: Poisson's constant for the strain along axis j when a load is exerted along axis i
G_{ij}: Shear moduls on plane ij

The anisotropic model has 12 parameters, three of which correspond to the elasticity modulus, whereas three are related to the shear modulus and six are related to Poisson's constant. Three of the parameters related to Poisson's constant are independent and the other three are dependent (ABAQUS User Manual, 2014).

In the cross-anisotropic model, the material properties are assumed to be on the same plane; however, the material behavior differs along the vertical axis (i.e., t axis) on this plane. In other words, the material behavior is assumed to be isotropic on plane p. In this model, the stress-strain formula is as follows (ABAQUS User Manual, 2014):

$$\begin{Bmatrix}\varepsilon_{11}\\ \varepsilon_{22}\\ \varepsilon_{33}\\ \gamma_{12}\\ \gamma_{13}\\ \gamma_{23}\end{Bmatrix}=\begin{bmatrix}\frac{1}{E_p} & \frac{-\nu_p}{E_p} & \frac{-\nu_{tp}}{E_t} & 0 & 0 & 0\\ \frac{-\nu_p}{E_p} & \frac{1}{E_p} & \frac{-\nu_{tp}}{E_t} & 0 & 0 & 0\\ \frac{-\nu_{pt}}{E_p} & \frac{-\nu_{pt}}{E_p} & \frac{1}{E_t} & 0 & 0 & 0\\ 0 & 0 & 0 & \frac{1}{G_p} & 0 & 0\\ 0 & 0 & 0 & 0 & \frac{1}{G_t} & 0\\ 0 & 0 & 0 & 0 & 0 & \frac{1}{G_t}\end{bmatrix}\begin{Bmatrix}\sigma_{11}\\ \sigma_{22}\\ \sigma_{33}\\ \sigma_{12}\\ \sigma_{13}\\ \sigma_{23}\end{Bmatrix}$$

where

G_p: Shear modulus on plane p
G_t: Shear modulus on the plane perpendicular to plane p

This model has seven parameters, five of which are independent.

The five material constants of the cross-anisotropic elasticity

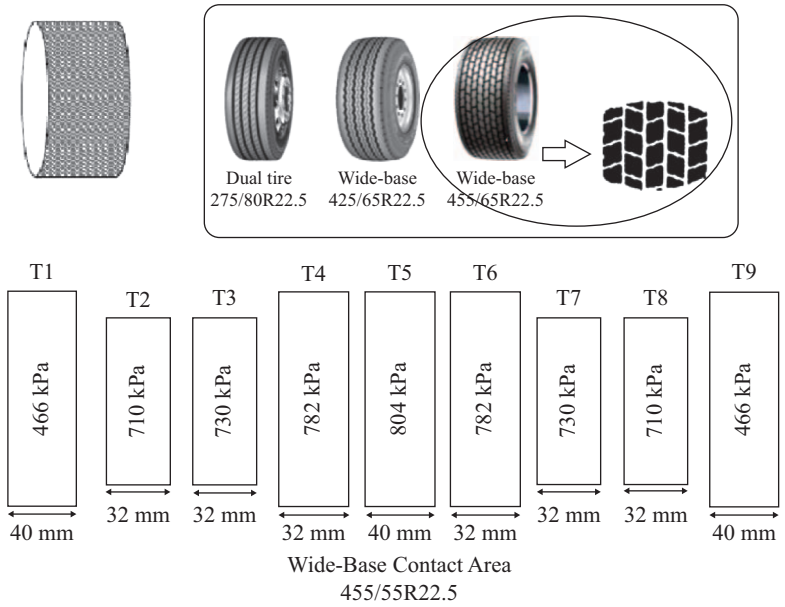

Fig. 3. Modeled tires and contact area.

are E_v, E_h, υ_{vh}, υ_{hh}, and G_{vh}: E_v and E_h are respectively the elastic moduli in the vertical and horizontal directions, υ_{vh} and υ_{hh} are respectively the Poisson's ratios for vertical-horizontal and horizontal-horizontal responses, and G_{vh} is the shear modulus along the vertical plane. Hooke's law for the crossanisotropic case can be expressed as follows:

$$\Delta\varepsilon_x = \frac{1}{E_h}\Delta\sigma_x - V_{hh}\frac{1}{E_h}\Delta\sigma_y - V_{vh}\frac{1}{E_v}\Delta\sigma_z \quad (1a)$$

$$\Delta\varepsilon_y = \frac{1}{E_h}\Delta\sigma_y - V_{hh}\frac{1}{E_h}\Delta\sigma_x - V_{vh}\frac{1}{E_v}\Delta\sigma_z \quad (1b)$$

$$\Delta\varepsilon_z = \frac{1}{E_h}\Delta\sigma_z - V_{vh}\frac{1}{E_h}\Delta\sigma_x - V_{vh}\frac{1}{E_v}\Delta\sigma_y \quad (1c)$$

where $\Delta\varepsilon_x$, $\Delta\varepsilon_y$, and $\Delta\varepsilon_z$ are normal strain increments and $\Delta\sigma_x$, $\Delta\sigma_y$, and $\Delta\sigma_z$ are normal stress increments.

The relationship among $\mu = \frac{v_{hh}}{v_{hv}}$, $m = \frac{G_{hv}}{E_v}$, and $n = \frac{E_h}{E_v}$ was applied to simplify the number of parameters in ABAQUS,

where

$$V_{hh} = 0.35,\ V_{hv} = 0.35$$

$$\frac{V_{vh}}{V_{hv}} = \frac{E_v}{E_h} = \frac{1}{n} \Rightarrow V_{vh} = \frac{0.35}{n} \Rightarrow 1 - V_{hh}^{\,2} - 2V_{vh}\cdot V_{hv} - 2V_{vh}\cdot V_{hv}\cdot V_{hh} > 0$$

$$1 - 0.35^2 - 2(0.35)\left(\frac{0.35}{n}\right) - 2(0.35)(0.35)\left(\frac{0.35}{n}\right) > 0 \Rightarrow n > 0.38 \quad (2)$$

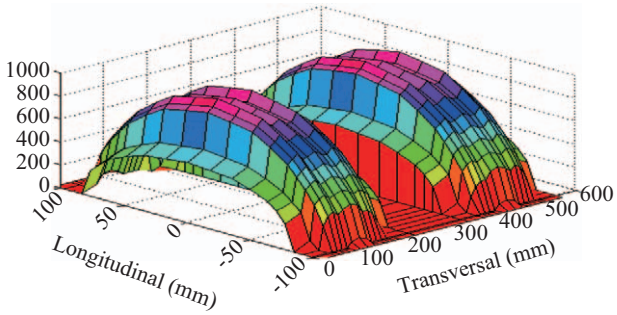

Fig. 4. Vertical contact stress distribution as predicted through numerical simulation.

The analysis was performed using various modulus ratios ($n = \frac{E_h}{E_v} = 0.5, 0.6, 0.7, 0.8, 0.9, 1$). In numerous studies, the value of the parameter m has been applied within the range of 0.35-0.40 (Tutumluer, 1995; Brown, 1996); in the present study, this ratio value was $m = \frac{G_{hv}}{E_v} = 0.40$.

The 3D FE models were developed to simulate the loading pattern for wide-base tire (i.e., 455/55R22.5) configurations (Fig. 3). During load movement, the stress transmitted to the pavement varied, the maximum (minimum) of which was expected to be at the center (edges). Two approaches were considered to simulate the longitudinal stress distribution underneath the tire. The first method involved simulating the modeled stress distributions of a simulated a two-contact body; the data were provided by the manufacturer of the various tire assemblies investigated herein. Fig. 4 shows the stress distribution, as determined by the manufacturer, for wide-

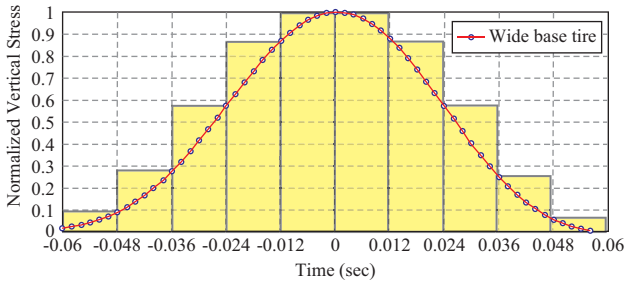

Fig. 5. Measured load amplitude function for the wide-base configurations.

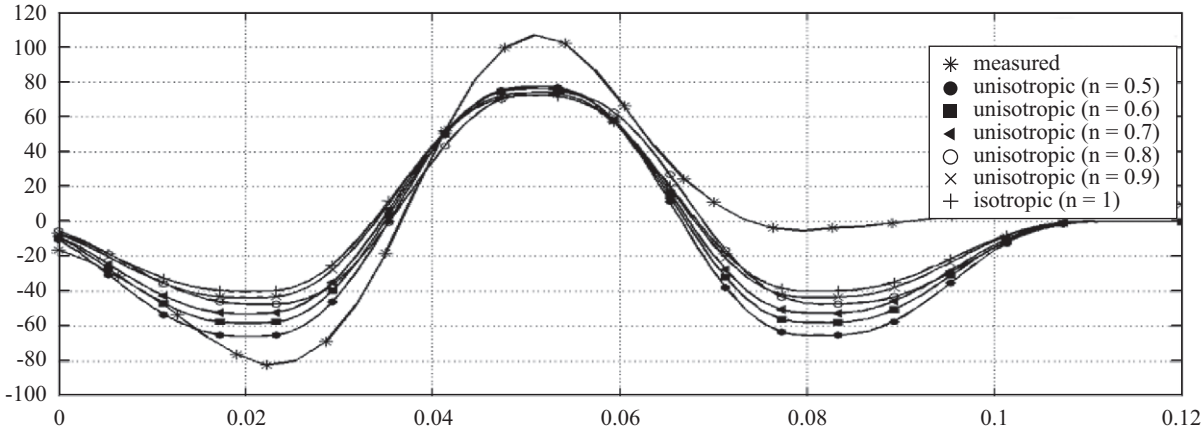

Fig. 6. Comparison between measured and calculated longitudinal strain at the bottom of the wearing surface.

base and dual tires, respectively. As shown in the figure, the stress was estimated to be relatively constant throughout the length of the tire footprint, dropping sharply at the edges. The second method involved considering the measured vertical stress in the field proximal to the surface (depth = 38.1 mm), representing the longitudinal vertical stress. In this case, vertical stress measurements at the bottom of the wearing surface for wide-base tires were discretized into small rectangular shapes at the Virginia Smart Road test-bed facility. The vertical stress was first normalized relative to the maximum recorded value. The normalized vertical stress was then multiplied by the average tire pressure measured on each tire tread. The maximum pressure was used in determining the maximum segments of the normalized histogram. Fig. 5 illustrates this modeling process for the wide-base tires. Notably, the loading time was found to increase with depth; moreover, for the loading time at a depth of 38.1 mm to be representative of the surface loading time, some approximations were applied. The advantage of the second method over the first one is that the measured vertical stress was derived from of the entire stress field at the surface, representing the actual stress transmitted to the pavement. By contrast, the first method required the simulation of the lateral stresses (i.e., longitudinal and transverse) to be completely accurate, which was not considered in this study.

The developed FE models were calibrated and validated using measurements obtained during the experimental program at the Virginia Smart Road test-bed facility. The experimental results were adjusted to a reference temperature (25°C) on the basis of a shift function. Fig. 6 shows a comparison of the measured and calculated longitudinal strains at the bottom of the HMA at 24.1 km/h. The tire inflation pressure was kept constant at 720 KPa during testing (Al-Qadi et al., 2004a). The FE model results were in high agreement with the field measurements. The developed 3D FE model appeared capable of predicting pavement responses at both simulated loading amplitudes.

III. NUMERICAL RESULTS

In the first part of this study, in which the ABAQUS and KENLAYER elastic systems were compared, three parameters were considered: the amount of load from passing vehicles, the elasticity modulus of the subgrade layer, and the elasticity modulus of the other layers. The amount of stress, strain and vertical displacement obtained using ABAQUS and KENLAYER software were compared statistically. In the second part of this study, three critical parameters, namely the amount of load from passing vehicles, the vehicle speed, and the elasticity modulus of the subgrade layer, were considered to determine the amount of stress, strain and displacement under 120 pavement conditions by applying the FE method with ABAQUS to obtain isotropic and anisotropic models. The values obtained from the stress, strain, and displacement analyses, as well as the results

Table 2. Stress *t* test results.

Software	N	Mean (KPa)	Std. Deviation	Std. Error Mean	T	Df	Sig
KENLAYER	200	*244.9*	*246.9*	*17.4*	*0.25*	*395.9*	*0.802*
ABAQUS	200	238.5	265.7	18.8			

Table 3. Strain *t* test results.

Software	N	Mean (m/m)	Std. Deviation	Std. Error Mean	T	Df	Sig
KENLAYER	200	*0.00005*	*0.000032*	*0.0000023*	*2.78*	*398.9*	*0.030*
ABAQUS	200	0.00004	0.000032	0.0000022			

Table 4. Displacement *t* test results.

Software	N	Mean (mm)	Std. Deviation	Std. Error Mean	T	Df	Sig
KENLAYER	200	*0.128*	*0.045*	*0.005*	*-1.92*	*198.1*	*0.056*
ABAQUS	200	0.141	0.052	0.005			

Table 5. Stress ANOVA results.

Stress	Sum of Squares	Df	Mean Square	F	Sig.
Between Groups	1155404.1	5	231080.8	0.573	0.72
Within Groups	5.775E8	1433	402997.1		
Total	5.787E8	1438			

of a failure analysis, were statistically analyzed using SPSS. Significant parameters were subjected to a regression analysis to control the effects of individual parameters. Significant parameters indicate a significant relationship between variables; in a model containing logicaly related variables, the *P* value should be lower than 0.05 to achieve statistical significance. Otherwise, the difference between the parameters is regarded as statistically nonsignificant. SPSS was used to examine the analysis results and pavement design.

1. Statistical Analysis of Pavement

In the first part of this study, SPSS was used for a statistical analysis of the stress, strain, and displacement by applying a *t* test, the results of which are shown in Tables 2-4, respectively. The tables indicate that the amount of stress was $T(395.87) = 0.251$, $P > 0.05$, the amount of strain was $T(398.9) = 2.781$ ($P > 0.01$), and the vertical displacement was $T(198.1) = -1.922$ ($P > 0.05$). Therefore, the differences in the average stress, displacement, and strain between the ABAQUS and KENLAYER applications were nonsignificant at all levels (Fig. 7).

In the second part of this study, SPSS was used to investigate the relationship between the pavement structure analysis results for both the isotropic and anisotropic characteristics of the pavement systems by conducting inferential statistical tests. First, a one-way analysis of variance (ANOVA) was performed to examine the displacement, stress, and strain in the isotropic ($n = 1$) and anisotropic ($n = 0.5$, 0.6, 0.7, 0.8, and 0.9) models. Table 5 indicates that the stress analysis result was $F(1438) = 0.573$, ($P > 0.05$), whereas Tables 6 and 7 show that the strain analysis results were $F(1438) = 3.066$, ($P < 0.01$) and Table 8 indicates that the vertical displacement analysis result was $F(719) = 0.468$, ($P > 0.05$); thus, no significant difference was observed between the average stress and displacement in the isotropic and anisotropic models, but a significant difference was observed between the average strain in the isotropic and anisotropic models. The average values are shown in Fig. 8.

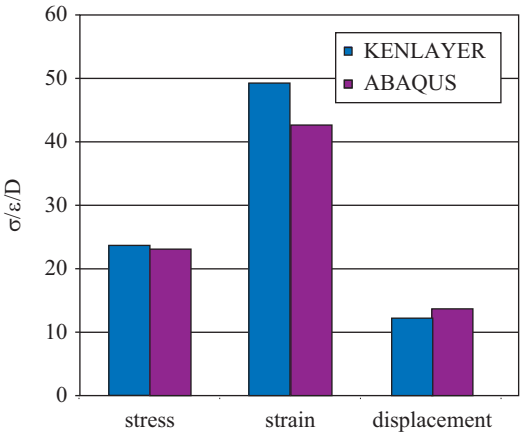

Fig. 7. Mean value.

Subsequently, the vertical and longitudinal stress and strain parameters were separately analyzed; the results are described as follows.

Table 6. Strain ANOVA results.

Strain	Sum of Squares	Df	Mean Square	F	Sig.
Between Groups	70657.8	5	14131.57	3.07	0.009
Within Groups	6605056.9	1433	4609.25		
Total	6675714.8	1438			

Table 7. Displacement ANOVA results.

Displacement	Sum of Squares	Df	Mean Square	F	Sig.
Between Groups	0.070	5	0.014	0.47	0.800
Within Groups	21.218	714	0.030		
Total	21.287	719			

Table 8. Vertical stress ANOVA results.

Vertical stress	Sum of Squares	Df	Mean Square	F	Sig.
Between Groups	919623.581	5	183924.7	0.34	0.88
Within Groups	3.791E8	714	530936.6		
Total	3.800E8	719			

Table 9. Longitudinal stress ANOVA results.

Longitudinal stress	Sum of Squares	Df	Mean Square	F	Sig.
Between Groups	1535828.63	5	307165.7	1.170	0.32
Within Groups	1.875E8	714	262549.2		
Total	1.890E8	719			

Table 10. Vertical strain ANOVA results.

Vertical Strain	Sum of Squares	Df	Mean Square	F	Sig.
Between Groups	349.259	5	69.852	0.015	1.00
Within Groups	3327378.88	714	4660.195		
Total	3327728.14	719			

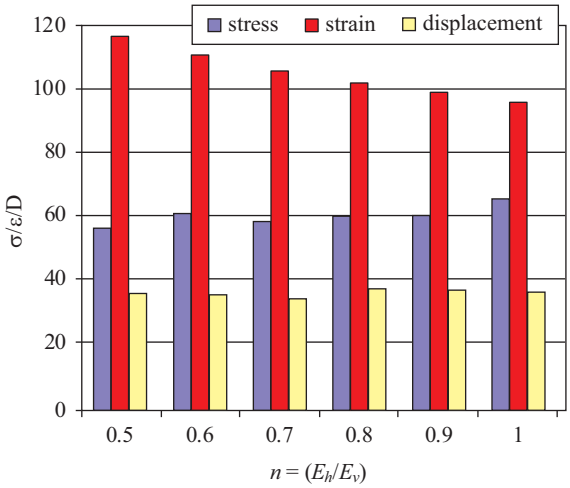

Fig. 8. Mean values of stress, strain, and displacement.

In this stage, a one-way ANOVA was used to compare the vertical compressive stress at the center of the load application at the top of the subgrade layers of the two pavement systems. As shown in Table 8, the result was $F(719) = 0.34$ ($P > 0.05$); thus, the difference in the vertical compressive stress between the isotropic and anisotropic models was nonsignificant.

In the third stage, a one-way ANOVA was also employed to compare the differences in the longitudinal tensile strain at the bottom of the HMA layer between the isotropic and anisotropic models; Table 9 presents the results with a confidence level of 95%. Statistically, no significant difference was observed in the mean longitudinal tensile strain at the bottom of the HMA layer between the isotropic and anisotropic pavement systems.

In the fourth stage, a one-way ANOVA test was again used to compare the vertical compressive strain at the top of the subgrade layer; the results are presented in Table 10. The FE analysis results of the modeling pavement system evidenced no significant difference in the mean compressive strain between the isotropic and anisotropic materials; $F_{(719)} = 0.015$ ($P > 0.05$).

In the final stage, a one-way ANOVA was employed to

Table 11. Longitudinal strain ANOVA results.

Longitudinal strain	Sum of Squares	Df	Mean Square	F	Sig.
Between Groups	127628.593	5	25525.71	8.72	0.000
Within Groups	2087817.36	714	2924.114		
Total	2215445.95	719			

Table 12. Means and significant model parameters for longitudinal strain.

n(I)-n(J)		Mean Difference (I-J)	Std. Error	Sig.	95% Confidence Interval	
					Lower	Upper
0.5	0.6	12.0414	6.98106	0.516	-7.9071	31.9893
	0.7	21.51847*	6.98106	0.026	1.5703	41.4667
	0.8	28.34762*	6.98106	0.001	8.3994	48.2958
	0.9	34.22017*	6.98106	0.000	14.2720	54.1684
	1.0	39.09583*	6.98106	0.000	19.1476	59.0440
0.6	0.5	-12.04114	6.98106	0.516	-31.9893	7.90071
	0.7	09.47733	6.98106	0.752	-10.4709	29.4255
	0.8	16.30648	6.98106	0.181	-3.6417	36.2547
	0.9	22.17903*	6.98106	0.019	2.2308	42.1272
	1.0	27.05469*	6.98106	0.002	7.1065	47.0029
0.7	0.5	-21.51847*	6.98106	0.026	-41.4667	-1.5703
	0.6	-09.47733	6.98106	0.752	-29.4255	10.4709
	0.8	06.82914	6.98106	0.925	-13.1191	26.7773
	0.9	12.70170	6.98106	0.454	-7.2465	32.6499
	1.0	17.57736	6.98106	0.120	-2.3708	37.5256
0.8	0.5	-28.34762*	6.98106	0.001	-48.2958	-8.3994
	0.6	-16.30648	6.98106	0.181	-36.2547	3.6417
	0.7	-06.82914	6.98106	0.925	-26.7773	13.1191
	0.9	05.87256	6.98106	0.960	-14.0756	25.8208
	1.0	10.74822	6.98106	0.639	-9.2000	30.6964
0.9	0.5	-34.22017*	6.98106	0.000	-54.168	-14.2720
	0.6	-22.17903*	6.98106	0.019	-42.1272	-2.2308
	0.7	-12.70170	6.98106	0.454	-32.6499	7.2465
	0.8	-05.87256	6.98106	0.960	-25.8208	14.0756
	1.0	04.87566	6.98106	0.982	-15.0725	24.8239
1.0	0.5	-39.09583*	6.98106	0.000	-59.0440	-19.147
	0.6	-27.05469*	6.98106	0.002	-47.0029	-7.1065
	0.7	-17.57736	6.98106	0.120	-37.5256	2.3708
	0.8	-10.74822	6.98106	0.639	-30.6964	9.2000
	0.9	-04.87566	6.98106	0.982	-24.8239	15.0725

compare the longitudinal tensile strain under load at the bottom of the HMA layer between the isotropic and anisotropic models. The analysis results in Tables 11 and 12 show that $T_{(719)}$ = 8.729 ($P < 0.01$); no significant difference was observed in the longitudinal tensile strain at a confidence level of 99% between the isotropic ($n = (E_h/E_v) = 1$) and anisotropic ($n = (E_h/E_v) = 0.5$, 0.6, 0.7, 0.8, and 0.9) models. Thus, the mean strain did not differ significantly between the isotropic and anisotropic models.

2. Statistical Analysis of Pavement Damage

Pavement structure deterioration may occur because of the adverse effects of environmental factors, traffic loading, construction deficiency, and poor maintenance (Huang, 2005). To account for the most severe types of load-associated pavement distress, two failure mechanisms were considered in this study: fatigue cracking and subgrade rutting.

Fatigue cracking is caused by repeated exposure to axle loads

Table 13. Fatigue cracking ANOVA results.

fatigue cracking	Sum of Squares	Df	Mean Square	F	Sig.
Between Groups	2.090E13	5	4.180E12	6.00	0.000
Within Groups	5.850E13	84	6.964E11		
Total	7.940E13	89			

Table 14. Means and significant model parameters for fatigue cracking.

n(I)-n(J)		Mean Difference (I-J)	Std. Error	Sig.	95% Confidence Interval	
					Lower	Upper
0.5	0.6	-89060.000	3.0472E5	0.771	-695033	516913
	0.7	-3.18467E5	3.0472E5	0.299	-924440	287506
	0.8	-5.75530E5	3.0472E5	0.062	-1.181E6	30443.5
	0.9	-8.82423E5	3.0472E5	0.005	-1.488E6	-276449
	1.0	-1.3948E6*	3.0472E5	0.000	-2.000E6	-788919
0.6	0.5	89060.000	3.0472E5	0.771	-516913	695033
	0.7	-2.29407E5	3.0472E5	0.454	-835380	376566
	0.8	-4.86470E5	3.0472E5	0.114	-1.092E6	119503
	0.9	-7.9336E5	3.0472E5	0.011	-1.39E6	-187389
	1.0	-1.3058E6*	3.0472E5	0.000	-1.91E6	-699859
0.7	0.5	3.18467E5	3.0472E5	0.299	-287506	924440
	0.6	2.29407E5	3.0472E5	0.454	-376566	835380
	0.8	-2.57063E5	3.0472E5	0.401	-863036	348910
	0.9	-5.63957E5	3.0472E5	0.068	-1.169E6	42016
	1.0	-1.0764E6*	3.0472E5	0.001	-1.682E6	-470453
0.8	0.5	5.75530E5	3.0472E5	0.062	-30443	1.1815E6
	0.6	4.86470E5	3.0472E5	0.114	-119503	1.0924E6
	0.7	2.57063E5	3.0472E5	0.401	-348910	863036
	0.9	-3.06893E5	3.0472E5	0.317	-912866	299080
	1.0	-8.1936E5*	3.0472E5	0.009	-1.42E6	-213389
0.9	0.5	8.82423E5	3.0472E5	0.005	-54.168	1.4884E6
	0.6	7.93363E5	3.0472E5	0.011	-42.1272	1.3993E6
	0.7	5.63957E5	3.0472E5	0.068	-32.6499	1.1699E6
	0.8	3.06893E5	3.0472E5	0.317	-25.8208	912866
	1.0	-5.12470E5	3.0472E5	0.096	-15.0725	93503
1.0	0.5	1.3948E6*	3.0472E5	0.000	788919	2.000E6
	0.6	1.3058E6*	3.0472E5	0.000	699859	1.911E6
	0.7	1.0764E6*	3.0472E5	0.001	470453	1.682E6
	0.8	8.1936E5*	3.0472E5	0.009	213389	1.425E6
	0.9	5.12470E5	3.0472E5	0.096	-93503	1.118E6

that are usually lower than the strength of the material. This type of pavement distress is progressive localized damage caused by fluctuating stress and strain in the material as well as by the buildup of irrecoverable strain (Hsu and Tseng, 1996). Fatigue cracking usually starts at the bottom of the HMA layer, which is the location of the greatest tensile strain in the case of fully bonded conditions between multiple HMA layers. Fatigue cracking can also start at the bottom of the individual HMA layers if unbonded or friction conditions exist. The following transfer function was employed to determine the number of cycles required to cause fatigue cracking (Adu-Osei, 2000):

$$N_f = 0.0796\ (\varepsilon_t)^{-3.291}\ (E)^{-0.854} \tag{3}$$

where

N_f: Number of repetitions required for fatigue cracking to occur

ε_t: Tensile strain at the bottom of the HMA layers (i.e., microstrain)

Table 15. Subgrade rutting ANOVA results.

Subgrade Rutting	Sum of Squares	Df	Mean Square	F	Sig.
Between Groups	1.006E21	5	2.012E20	0.23	0.945
Within Groups	9.636E22	114	8.453E20		
Total	9.737E22	119			

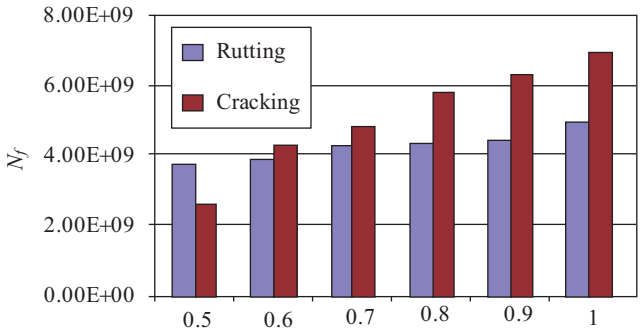

Fig. 9. Average N_f based on fatigue cracking and subgrade rutting.

E: Resilient modulus of HMA (i.e., psi)

Subgrade rutting is a longitudinal depression in the wheel path, which occurs because of excessive densification of the subgrade materials and lateral movement of the portion of the pavement layers above the subgrade layer. In the model presented by the Asphalt Institute, the strain on top of the subgrade layer is considered as critical strain. This model of the number of load repetitions required for subgrade rutting failure to occur is expressed as follows (Adu-Osei, 2000):

$$N_f = 1.365 \times 10^{-9} (\varepsilon_c)^{-4.477} \quad (4)$$

where

N_f: Number of repetitions required for subgrade rutting failure to occur
ε_c: Compressive strain on top of the subgrade layer

Finally, this study evaluated the effect of the anisotropic behavior of materials on the performance of flexible pavement according to the fatigue cracking of the asphalt surface layer and permanent deformation potential of the subgrade layers. An ANOVA was again used for this evaluation. Tables 13 and 14 present the ANOVA results for the fatigue cracking evaluation of the pavement systems. Table 14 shows a significant difference in N_f between the isotropic (n = 1) and anisotropic ($n = E_v$ = 0.5, 0.6) models, indicating that when the anisotropic characteristics of the materials is considered in the modeling of the pavement structure, the expected service life of the pavement system is shorter than when the anisotropic characteristics are not considered. Fig. 9 shows a comparison of the N_f values based on fatigue damage criteria and permanent deformation potential of the subgrade layers for the anisotropic modeling of the pavement structure.

A statistical analysis of fatigue cracking was performed using an ANOVA; the results are shown in Table 15. The result of $F_{(119)} = 0.23$ ($P > 0.05$) shows that no significant difference existed among the results of the damage analysis between the isotropic and anisotropic models at a scale of N_f before requiring pavement replacement; therefore, Fig. 9 shows no difference between the average N_f values before the occurrence of fatigue cracking in the isotropic and anisotropic models.

IV. CONCLUSIONS

The conclusions of this analytical study are as follows:

(1) Because the results of the linear elastic analysis of the FEs were similar to those derived from the theory of multilayer systems, and because the averages of the two methods do not differ significantly, the simple and fast method of the multilayer theory can be employed, rather than the expensive and time-consuming FE method for linear elastic analysis of flexible pavements.
(2) Because various pavement specifications can be modeled using the FE method, it is appropriate for pavement analysis under certain conditions such as when examining viscoelastic or anisotropic specifications or when considering the temperature effect on pavement behavior. However, the FE method is not a suitable substitute for analyzing the material properties.

The ANOVA results revealed the following:

(1) No significant difference was observed in the mean vertical compressive stress or vertical compressive strain at the top of the pavement structures between the isotropic and anisotropic systems.
(2) Significant differences were observed in the mean tensile strain induced at the bottom of the asphalt surface layer of the pavement structures between the isotropic and anisotropic systems.
(3) The magnitude of the induced tensile strain at the bottom of the asphalt surface layer is larger for pavement structures modeled as anisotropic systems.
(4) Based on the fatigue cracking criteria, a significant difference exists in the expected service life of pavement structures between isotropic and anisotropic systems. Isotropic modeling of a pavement system predicts a longer expected service life.

(5) According to the permanent deformation criteria, no significant difference exists in the expected service life of pavement structures between isotropic and anisotropic systems.

ACKNOWLEDGEMENTS

This work was financially supported by Islamic Azad University, Marivan Branch, Marivan, Iran.

REFERENCES

ABAQUS. (2014). Finite Element Computer Program, Users Manual. Version 6.14-4, Karlsson and Sorensen, Inc., Pawtucket, USA.

Adu-Osei, A., R. L. Lytton and D. N. Little (2000). System Identification Method for Determining the Anisotropic Resilient Properties of Unbound Aggregates. Symposium Unbound Aggregates in Roads (UNBAR5), University of Nottingham Nottingham, England, June 21-23.

Adu-Osei, A. (2000). Characterization of Unbound Granular Base", Ph.D. Dissertation, Texas A&M University, College Station, TX.

Al-Qadi, I. L., A. Loulizi, I. Janajreh and T. E. Freeman (2002). Pavement response to dual and new wide-base tires at the same tire pressure. J. Transp. Res. Board 1806, 38-47 TRB.

Al-Qadi, I. L., A. Loulizi, M. A. Elseifi and S. Lahouar (2004a). The Virginia Smart Road: The impact of pavement instrumentation on understanding pavement performance. J. Assoc. Asphalt Pavement Technol. 73, 427-465.

Al-Qadi, I. L., M. A. Elseifi and P. J. Yoo (2004b). Pavement damage to different tires and vehicle configuration. Michelin Americas Research and Development Corporation Ichelin Americas Research and Development Corporation 515 Michelin Road PO BOX 1987Greenville, SC 29602-1987 the Roadway Interastructure Group Virginia Tech Transportation Institute350 Transportation Research Plaza Blacksburg, VA 24060.

Al-Qadi, I. L., P. J. Yoo, M. A. Elseifi and I. Janajreh (2005). Effects of tire configurations on pavement damage. Paper No. 58 presented at the 2005 Annual Meeting of the Association of Pavement Technologists and accepted for publication by the J. Assoc. Asphalt Pavement Technol.

Brown, S. F., M. P. O'Reilly and J. W. A. Pappin (1989). Repeated Load Triaxial Apparatus for Granular Materials. In Unbound Aggregates in Roads, R. H. Jones and A. R. Dawson (Eds), Butter worths, London, 143-158.

Brown, S. F. (1996). Soil mechanics in pavement engineering. Geotechnique 46(3), 383-426.

Chan, F. K. and S. F. Brown (1994). Significance of principal stress rotation in pavements. 13th International Conference on Soil Mechanics and Foundation Engineering, Delhi 4, 1823-1826.

Hsu, T. W. and K. H. Tseng (1996). Effect of rest periods on fatigue response of asphalt concrete mixtures. Journal of Transportation Engineering, American Society of Civil Engineering 122(4), 316-322.

Huang, Y. H. (2005). Pavement Analysis and Design, 2nd Edition . Prentice Hall. Englewood Cliffs. NJ.

Kolisoja, P. (1997). Resilient Deformation Characteristics of Granular Materials, Ph.D. Dissertation, Tampere University of Technology, Tampere, Finland.

Oda, M., S. Nemat-Nasser and J. Konish (1985). Stress-induced anisotropy in granular masses. Soils and Foundations 25, 85-97.

Oda, M. and N. Nakayama (1989). Yield function for soil with anisotropic fabric. Journal of Engineering Mechanics, ASCE 15, 89-104.

Tutumluer, E. (1995). Predicting behavior of flexible pavements with granular bases, Ph.D. Dissertation, School of Civil Environmental Engineering, Georgia Institute of Technology, Atlanta.

Tutumluer, E. (1998). Anisotropic behavior of unbound aggregate bases. In Proc., 6th Annual Symposium, International Center for Aggregate Research, St. Louis, 11-33.

Tutumluer, E., D. N. Little and S. H. Kim (2003). Validated model for predicting field performance of aggregate base courses. Transportation Research Record 1837, TRB, National Research Council, Washington, DC, 41-49.

Underwood, S., H. Heidari and R. Kim (2005). Experimental investigation of anisotropy in asphalt concrete. Transportation Research Record 1929, TRB, National Research Council, Washington, DC, 238-247.

Wagoner, M. and F. Braham (2008). Anisotropic behavior of hot-mix asphalt at low temperatures. Transportation Research Record 2057, TRB, National Research Council, Washington, DC, 83-88.

Wang, L. B. and L. R. Hoyos (2004). Anisotropic properties of asphalt concrete: characterization and implications in pavement design and analysis. Transportation Research Record 2083, TRB, National Research Council, Washington, DC., 2-3.